Progress in halide-perovskite nanocrystals with near-unity-photoluminescence quantum yield

Andrés F. Gualdrón-Reyes[1], Sofia Masi[1], and Iván Mora-Seró[1,*,@]

[1]Institute of Advanced Materials (INAM), Universitat Jaume I (UJI), Avenida de Vicent Sos Baynat, s/n, 12071 Castellón de la Plana, Spain.

*Correspondence: sero@uji.es (I. Mora-Seró) @IvanMoraSero

Abstract

Colloidal halide perovskite nanocrystals (PNCs) are an outstanding case study due to their remarkable optical features, such as a high photoluminescence quantum yield (PLQY), tunable band gap, and a narrow emission. Despite the impressive first reports of PLQY beyond 70% for PNCs, it has been observed that PLQY is limited by a defective structure, due to the labile interaction between the organic capping ligand and inorganic core. In this line, structural defects acting as trap states are the key factor to limit not just PNCs PLQYs but also their stability. In this review, we present the most studied, common, and alternative protocols to fully compensate for surface defects, mainly halide vacancies and the loss of protective capping ligands, as well as how increase their stability and PLQY up to100%.

Keywords: perovskite nanocrystals; photoluminescence quantum yield; synthetic protocols; ligand passivation; defect suppression; high-quality materials

Defective perovskite nanocrystals after synthesis

Halide perovskite nanocrystals (PNCs) with $APbX_3$ formulation (A= Cs^+, FA^+; formamidinium, MA^+; methylamonium, X = Cl, Br, I and corresponding mixtures) have received growing interest in optoelectronics, photovoltaics, and analogous solar-driven processes as photocatalysis, extending their applicability during recent years. The outstanding photophysical properties of PNCs such as tunable band gaps covering a broad UV-Vis-IR region [1, 2], narrow **full width at half maximum** (FWHM) photoluminescence (PL) [3], stability in room ambient conditions [4, 5], versatile surface chemistry and facile processability [6-8], have triggered diverse

studies to prepare PNC colloidal solutions for efficient multicolor light-emitting diodes (LEDs) [9-13], perovskite quantum dot solar cells (QDSSCs) [14-18], and conduct oxidation/reduction reactions on model systems [2, 19, 20], solar fuel generation [21, 22], and solar synthesis [23]. Since the first report provided by Perez Prieto and co-workers [24] and Kovalenko and co-workers[1] on the synthesis of $CH_3NH_3PbBr_3$ and $CsPbX_3$ PNCs in 2014 and 2015, respectively, research in the field of PNCs has demonstrated that improvement of the above properties is defined by the quality of the synthesized PNCs, established by estimating their **photoluminescence quantum yield** (PLQY) [5]. After six years of continuous studies on the intrinsic properties of PNCs, it has been deduced that these materials are denoted as "high-quality" when their PLQY is >90% [5, 25, 26]. This means that the **radiative recombination** mechanism requires the material to be as trap-free as possible and mostly dictates the optoelectronic features of PNCs [27].

In this way, PNCs are commonly preferred as promising light-emitters with high color quality over analogous systems such as 3D perovskite bulk films, where a lower PLQY is usually reported [28]. Although, computational studies have demonstrated that the different defects density in bulk perovskite and PNCs is not enough to explain the difference in the PLQY between them, other main aspects such as the interaction with ligands and solvent, and the location of the defects lead to the control of the surface passivation and in turn of the PLQY, are more easily maximized in the PNCs [29]. Indeed, bulk films also suffer of ion migration promoted in the grain boundaries, favoring the non-radiative recombination dynamics mediated by defects and low-stability [30]. However, the presence of surface-passivating organic ligands, and the spatial confinement of PNCs reduce the emergence of ion migration-mediated defects, improving their PL properties [31]. Interestingly, PNCs colloidal solutions have been used as an additive during bulk film processing [32, 33], generating a reduction of defects in bulk by passivating carrier traps through ionic species provided by PNCs and surface passivation by ligand anchoring [34].

Therefore, the fact that high-quality PNCs, with high PLQY, show a low density of intra band gap carrier traps, reducing the non-radiative recombination pathway into PNCs layers, favoring that LEDs reach higher external quantum efficiencies (EQE) greater than 20% [13, 35, 36]. The reduction of defects has also hindered the loss of carriers during their transportation into high efficient QDSSCs with photoconversion efficiencies of 16.6% [18], and induce better electron extraction and enhanced photocurrent in photodetectors, with high photoresponsivity/detectivity of $1.4x10^8$ AW^{-1}/ 4.72×10^{15} Jones at an incident light 430 nm [37]. However, despite the impressive PLQYs of the first reports, the fact that the PLQYs of Cs-, FA-PbX_3 PNCs does not reach unity in many cases [38-41] is clear evidence that these materials are not fully defect-free, and in certain cases, the non-radiative channel is also open for deteriorating their optical properties and long-term stability.

In this context, diverse research groups agree that the quality of PNCs depends mainly on the synthetic protocol used for material growth. The stoichiometric mixture of Cs_2CO_3, PbX_2, and long-chain **capping ligands** as oleic acid (OA) and oleylamine (OLA) during PNC synthesis, produces a degree of structural defects in the final product. Halide vacancies are the most well-recognized defects in the PNCs, and they are represented by the emergence of metallic lead, Pb^0 [42]. These undercoordinated Pb species are located in the PNC surface acting as **non-radiative recombination** centers for electron trapping [43, 44]. The generation of these defects has been also associated with difficulties in stabilizing the PNCs. During PNC preparation, OA and OLA are transformed into oleylammonium oleate, which is the main species for PNC stabilization [5, 45, 46]. Oleylammonium cations bind to halide anions of the PNCs as ionic pairs, promoting **surface passivation**. Unfortunately, a fraction of the ammonium ligand, now denoted as oleylammonium halide, can be easily detached from the PNC surface, giving place to halide defects [45, 47].

Through density functional theory calculations, Chen and co-workers[48] reported that the adsorption energy of the OLA-capped $CsPbI_3$ (4.599 eV) is lower than that of shorter-capping ligands covering the PNC surface as octylamine (OctA, 5.022 eV). In this case, the OctA (Lewis base ligand) preferentially coordinates with metal atoms of the surface. OctA-$CsPbI_3$ PNCs exhibited an increase in long-term stability for 6 months, with a PLQY~ 94%, reducing iodide defects and retaining the cubic phase, as stabilization of **perovskite black phase** is an additional advantage of the PNC synthesis [49]. Thus, the dynamic ligand binding nature is the initial step towards the stabilization and depends on the type of ligands, as well as on the PNC surface.

Clearly, additional strategies supporting the most common use of ammonium ligands, that maximize the radiative recombination pathway, along with the passivation of halide deficiency, are desirable to reach a 100% PLQY. In this review, we highlight the main approaches to achieve PNCs with 100% PLQY, based on the purification stage, surface post-synthetic treatments, partial Pb substitution/cation doping and modified synthetic routes to produce high-quality materials for perovskite-based technologies.

Purification of the perovskite nanocrystals

One of the main problems associated with PNCs is maintaining or improving of their optical and structural properties during isolation and purification steps following synthesis. Variations in the purification stage have been mostly considered in order to evaluate the quality of the final product [50-52]. On one hand, the addition of antisolvents to the crude reaction has been reported to decrease the PLQY of PNCs (from 70% to 30% for $CsPbBr_3$ and from 80% to 0% for $CsPbI_3$) caused by the detachment of a high amount of capping ligands from the PNC surface [48, 53, 54]. This leads to several issues such as PNC agglomeration, a wide particle size distribution (broad

PL FWHM) and thereby, the preference for the non-photoactive **yellow δ-phase** in the case of iodide perovskites [49, 51, 52]. However, the PNCs isolation in absence of antisolvents causes a high density of nanoparticles (NPs) to be dispersed in the supernatant, which is then discarded, reducing the product yield [51]. Therefore, the purification process to achieve a high amount of PNCs without altering their optical properties is still under study.

Experimental parameters such as the antisolvent nature, solvent:antisolvent volume ratio, and centrifuge rate and time also influence PNCs isolation. Zhang and co-workers [51] studied the compatibility of some PNCs such as $CsPbBr_3$, $CsPbI_3$, and some antisolvents with different polarity, as the case of methanol, 1-butanol, acetonitrile, acetone, methyl acetate (MeOAc), and ethyl acetate (EtOAc) (Figure 1a). Here, a centrifugation rate of 8000 rpm for 5 min and a 1:1 volume ratio of solvent:antisolvent were established. Then, PNCs were redispersed in hexane and centrifugate again at 8500 rpm for 5 min. At this point, the supernatant was recovered as a purified product. By measuring the PL spectra of purified PNCs (Figure 1b), and by comparing their optical features with a luminescent standard system like Rhodamine B, it was found that $CsPbBr_3$ was stable in all the antisolvents, reaching a PLQY >90% by washing with methanol and unity-PLQY after washing with acetonitrile. In the case of $CsPbI_3$ PNCs, highly polar antisolvents decrease the PLQY considerably, promoting the emergence of a yellow δ-phase and the loss of the optical properties.

Although the PLQY of PNCs using MeOAc and EtOAc is <70% (Figure 1b), these antisolvents are commonly chosen for a higher PNC product yield to facilitate their applications, especially in LEDs [55, 56]. On the other hand, Konstantatos and co-workers[57] proposed a facile route to enhance the photophysical properties of $FAPbBr_3$ PNCs synthesized with short-chain capping ligands as octylamine and octanoic acid: the simultaneous addition of OA and $PbBr_2$ to the redispersed material in toluene, prior to purification with MeOAc. The presence of OA removes the presence of PNC aggregates, while $PbBr_2$ provides an excess of Br^- anions to passivate the halide defects and strengthen the ligand binding in the PNC surface [57, 58]. This procedure affords purified $FAPbBr_3$ PNCs with a PL peak emission at 511 nm, FWHM = 22 nm, and PLQY around 90 ± 9% (Figure 1c). The improvement of PLQY was accompanied with a change in the PL dynamics of the PNCs, where the carrier lifetime was longer for purified materials compared with the as-synthesized ones (Figure 1d). This fact is associated to the reduction of the non-radiative recombination paths, providing efficient photoluminescence.

Surface restoration of the perovskite nanocrystals

Stronger ligand binding to perovskite core

One of the most recognized strategies to compensate for the loss of organic ligands from the shell life of the $CsPbBr_3$ PNCs is through post-synthetic treatment with quaternary ammonium salts, namely didodecyldimethylammonium bromide (DDAB) [53, 59, 60]. Compared with the linked OLA that shows a high likelihood of desorption, DDA^+ cations produce stronger binding with the negatively charge surface sites of the perovskite [61, 62]. This induces the formation of hydrophobic monolayers, increasing the long-term stability of the PNCs. The effect of DDAB can be also combined with the addition of $PbBr_2$, used for repairing the $PbBr_6$ octahedra from the Pb- or/and Br-deficiency. Bodnarchuk and co-workers [53] have incorporated both DDAB and DDAB+$PbBr_2$ to $CsPbBr_3$ colloidal solutions, which showed a low PLQY near to 60-70% before purification and 30-40% after purification, respectively. After post-synthetic treatment, the PLQY of the samples raised to 100%. As shown in Figure 2a, the visual brightness of the samples in the presence of DDAB or DDAB+$PbBr_2$ is increased, reflecting the enhancement of the optical features, and indicating that electron relaxation is performed radiatively. The surface modification does not have a marked impact on the PL peak position of the $CsPbBr_3$ PNCs, exhibiting an emission peak between 512-514 nm, with a PL FWHM between 18-20 nm (Figure 2b). In this line, the use of three-ligand surface engineering where octanoic acid is pivotal for improving the optoelectronic features of $CsPbBr_3$ PNCs [63], and the addition of zwitterionic ligands with strong binding to PNCs surface [64, 65] are also considered promising strategies to achieve an efficient defect passivation of PNCs surface.

Therefore, the addition of efficient capping ligands during synthesis has been considered to provide better protection of the PNC surface [66-69]. Shen and co-workers [70] introduced trioctylphosphine (TOP) as a capping agent to be mixed with PbI_2, in order of achieving PNCs with a more perfect structure and suppressed surface defects. In this case, lone-pair electrons from P atoms are donated to Lewis acid Pb^{2+} cations, forming a TOP.PbI_2 adduct to facilitate the PbI_2 dissolution and generate more efficient passivation. Accordingly, TOP-$CsPbI_3$ PNCs show narrow PL FWHM ~30 nm, reduced carrier trap density, and thereby, a 100% PLQY compared with the TOP-free material, exhibiting values between 78-84%. The suitable passivation of surface defects by TOP allows for control of the PNC size by varying the synthesis temperature (particle size), obtaining a stable unity-PLQY (Figure 2c). Simultaneously, the high-quality of TOP-$CsPbI_3$ PNCs is visible after washing with MeOAc and storing for one month, with a decrease of only around 15% of the initial PLQY value. In contrast, standard $CsPbI_3$ PNCs with lower initial PLQY display a marked decrease around 26% (Figure 2d), indicating of a poorer passivated surface in the time. In addition to the enhancement of PLQY, PNCs also shows a

change in its PL decay behavior after carrying out an efficient surface passivation (Figure 2e). Unlike defective PNCs with low PLQY, exhibiting PL decay with multiexponential character, PNCs with near-unity PLQY display transient PL kinetics close to single-exponential character. This fact indicates that non-radiative recombination sites are suppressed to maximize the radiative channel [68, 71].

Removal of unloaded defect sites – fixing the surface stoichiometry.

Alivisatos and co-workers [71] have demonstrated the enhancement of PL properties of $CsPbBr_3$ PNCs by using thiocyanate salts such as NH_4SCN or NaSCN, to repair a lead-rich PNC surface and extending the **carrier lifetime** into the material (Figure 2e). SCN^- species are able to remove excess Pb^0 formed during the synthesis, forming Pb-S bonds. This provides a suitable surface stoichiometry (Pb:Br =1:3) without causing structural changes in the nanoparticles. The removal of Pb^0 decreases the density of carrier traps in the PNCs [72], trendering the radiative PL decay more efficient. By comparing the optical properties of fresh and aged $CsPbBr_3$ PNCs samples before and after SCN^- treatment, PLQY was maximized: from 92 ± 2% to 99 ± 2% for the case of as-prepared PNCs, while aged ones showed an improvement from 63 ± 2% to 100 ± 3%. Ahmed and co-workers [44] have added $NaBF_4/NH_4BF_4$ to $CsPbBr_2Cl$ colloidal solutions, boosting the PLQY from 4 ± 1% to 96 ± 3%. Here, Pb^0 species are removed by using BF_4^- anions. On the other hand, $CsPbI_3$ PNCs with 100% PLQY has not been reached in the presence of salts (e.g., SCN^- or ZnI_2) [26, 72]. This is attributed to the high iodide lability, generating halide vacancies and a fast phase transformation (α- to δ-phase) [49]. Consequently, the effectiveness of the salt treatment decreases.

Partial Pb substitution – doping

The addition of metal halides, including metal doping during or after PNC synthesis has been studied with the goal of (i) tuning/enhancing the photophysical properties of the materials, and (ii) decreasing the fraction of Pb to push commercialization of perovskite-based technologies [25, 73, 74]. However, some metals can introduce new non-radiative paths for carrier recombination, quenching the PL of the host [75], while in other cases, no modifications in the optical features are observed just as in the absence of the metal substitute [76, 77]. However, some transition, rare-earth metals or lanthanides have been studied deeply to improve the optoelectronic properties of PNCs with better phase stability through dual metal-doping [78-80].

Ji and colleagues [81] have shown enhancement of PL properties of Mn^{2+}-doped $CsPbCl_3$ PNCs by adding $CdCl_2$ (100 μL of 33 mM $CdCl_2$) in ethanol as a post-synthetic treatment. Attending to the the PLQY of standard $CsPbCl_3$ is low (< 10%) [77, 82], Mn^{2+} energy levels are

introduced in the band gap of the PNCs, causing orange-red light emission and making more efficient the radiative carrier recombination dynamics. However, a maximum PLQY around 62% was achieved for the Mn:Pb molar ratio 3:1, due to the presence of high density of non-radiative recombination sites formed by atomic vacancies into $CsPbCl_3$ host. These species block the Mn^{2+} *d-d* transition, generating octahedra tilting of $PbCl_6$ units [77, 83]. Through PNC dual-surface passivation with Cd^{2+} and Cl^- vacancies are rapidly filled, reducing the octahedra distortion and providing a unity-PLQY (Figure 3a). This is accompanied with the lengthening of the PL lifetime, corroborating the reduction of non-radiative sites from the PNCs. Simultaneously, $CdCl_2$-Mn^{2+}-$CsPbCl_3$ PNCs are not affected by subsequent purifications (Figure 3b), only reducing ~11% from the initial PLQY. Because the ionic radius of Cd^{2+} (0.95 Å) is smaller than that of Pb^{2+} (1.19 Å), the Goldschmidt tolerance factor is increased, producing a less defective structure with higher phase stability [77, 84].

Furthermore, Gamelin and co-workers[85] have introduced Yb^{3+} cations into $CsPbCl_3$ PNCs (doping 5.2%), raising the PLQY above the 100% in the near-infrared (NIR) region. Taking advantage from $^2F_{5/2} \rightarrow {}^2F_{7/2}$ *f-f* emission of Yb^{3+}, which is an effective activator of quantum cutting (one high-energy photon is absorbed and then two-low energy photons are generated) [78, 86], the carrier transfer from the host is accelerated, improving the radiative relaxation of the modified $CsPbCl_3$. After Yb^{3+}-doping and varying the intensity of the excitation source (λ = 380 nm), the highest PLQY around 170% was achieved (Figure 3c). This value is the highest reported for these materials and closer to the theoretical 200% for the visible-to-NIR quantum cutting in presence of Yb^{3+}.

It has been demonstrated that the partial replacement of Pb by Sr during synthesis of $FAPb_{1-x}Sr_xI_3$ PNCs [87] or $CsPbI_3$[25] generates red-emitting materials with high-quality. As Sr^{2+} cations exhibit the same ionic radius as Pb^{2+} [25], it is expected that SrI_2 can easily substitute PbI_2 in the mixture reaction, producing less-toxic PNCs, keeping their intrinsic properties. After adding 7 at.% Sr into $FAPbI_3$ PNCs, **Schottky defects** were suppressed, favoring the radiative recombination pathway. Thus, the PLQY of pristine $FAPbI_3$ was maximized from 93% to 100%, showing a blue shift in the PL features (Figure 3d). Interestingly, the excess Sr content generates the alteration of stoichiometry of the precursors during the PNCs synthesis, opening the door to distinct morphologies with different PL properties. In addition, Sr doping also increases significantly the stability, preserving the 80% of the initial PLQY after 6.5 months.

Modified synthetic routes for synthesizing high-quality perovskite nanocrystals

One encouraging approach to prepare high-quality PNCs is through the ligand-assisted reprecipitation technique (LARP). This protocol is simpler, lower- cost, faster, and requires milder conditions, being suitable for organic nanomaterials [88, 89]. Pérez-Prieto and co-

workers[90] have synthesized $MAPbBr_3$ nanoplatelets with unity-PLQY, by preparing solutions containing certain amount of MABr, $PbBr_2$ and 2-adamantylammonium bromide (ADBr) in DMF. A highly green-luminescent material is obtained after adding the mixture in a poor solvent such as toluene under stirring. Considering that $MAPbBr_3$ PNCs shows a PLQY near to 93% when OctA is used, the incorporation of ADBr provides better coverage of the material surface, reaching an effective passivation and improving the PL properties. A recent strategy to achieve $MAPbBr_3$ PNCs with 100% PLQY is by adding a solution of $MABr/PbBr_2$/OctA in DMF in toluene by spray pyrolysis. Lin and co-workers [91] explain that this methodology guarantees a larger contact surface area and better mixing between the good and poor solvent, improving the crystallization of the material.

Meanwhile, Sum and co-workers[92] have repaired the surface defects of $MAPbBr_3$ PNCs in presence of benzyl alcohol (BnOH), through LARP. Here, BnOH is able to mediate the ligand coverage and influence the ligand binding motifs, unlocking unity- PLQY. After analyzing high-resolution XPS O 1s spectra of the as-prepared $MAPbBr_3$ samples with (Figure 4a) and without (Figure 4b) of BnOH, two different chemical environments of the carboxylate oxygen atoms from OA linked to the PNC surface were observed; region I associated to the bidentate chelating binding mode, while region III is ascribed to monodentate chelating binding mode (Figure 4c). Region II was attributed to O-H species absorbed during sample preparation. It was concluded that the bidentate mode promotes a stronger binding to the Pb^{2+} cations from the PNCs surface, reducing the density of carrier traps.

Interestingly, Kovalenko and co-workers [93] show a modification of the LARP protocol to prepare $MAPbBr_3$ PNCs, by introducing the amino acids (AAs) as L-lysine and L-arginine in presence of hexanoic acid. For this purpose, the α-amino group from both AAs were blocked with a protecting group based on tertbutyloxycarbonyl (tBoc), which (i) forces the selective bonding between the positively amine-groups from AAs and the PNCs core to produce an efficient passivation, and (ii) the blocked functional groups are then free to react with precursors in the mixture reaction to provide a more effective PNCs growth. In this context, tBoc-AAs offer the formation of highly blue-emissive PNCs (Figure 4d) with particle sizes < 6 nm, low size distribution and a PLQY up to 94 ± 5% (Figure 4e).

Other alternatives are based on synthetic routes using three precursors (each one for Cs, Pb and Br, respectively), where several bromide sources (such as TOP-Br_2, N-bromosuccinimide, trimethylsilyl bromide, benzoyl bromide, alkyl-ammonium bromides, ionic liquids, among others) [64, 94-99] are added independently from the lead precursor (lead acetate or lead oxide) for $CsPbBr_3$ synthesis. This method aims to reduce the stoichiometric excess of Pb used in the synthesis and source of halide vacancies, which activate non-radiative recombination pathways, as discussed above. However, its main limitation regards the achievement of highly emissive nanoparticles with a shape different from the classical nanocubes (i.e., nanorods). Improved

methods reported by Grisorio and co-workers[100] were investigated for controlling the shape and stability of $CsPbBr_3$ PNCs while maintaining their high emission efficiency, mainly by controlling the reaction kinetics.

Regarding to the hot-injection method, some modifications have been also performed to improve the quality of the PNCs. It has been demonstrated that the increase of OA/OLA concentration in the mixture reaction facilitates both the stabilization of lead halide during the synthesis and the PNCs growth at temperatures between 170-190 ºC [5]. Meanwhile, Pradhan and co-workers [97] have described a generic synthetic approach to inject oleylammonium halide salts into an amine/halide-free mixture reaction containing an equimolar ratio of Pb and Cs at high temperatures (220-260 ºC). Both modified routes ensure an efficient ligand surface passivation of PNCs with near-unity PLQY.

Attending to the overall strategies shown along the manuscript (summarized in Figure 5a), we observe that they have been widely studied in Br-PNCs and I-PNCs systems. However, the high halide deficiency generated by the dynamic binding of iodide anions in the PNCs surface [2] makes that some approaches lose effectiveness. In this sense, the nature of the halide affects the strategy in order to boost PLQY of PNCs to near to one values. Thus, new synthetic routes and partial Pb replacement are suitable for reaching I-PNCs with high quality. On the contrary, the strong complexion affinity of the Pb-Br bond makes that Br-PNCs show a more tolerant-to-defect structure. This fact allows us to understand why the abovementioned strategies (mainly ligand passivation and salt treatments) are more effective in Br-PNCs to suppress their surface defects and reach 100% PLQY more easily. Lastly, the inclusion of metal chloride salts and doping are established as the most reported approaches to promote defect passivation of Cl-PNCs. By considering that Cl-vacancies are associated to intra band gap deep states compared with Br- and I-vacancies (shallow states) [68], we believe that the reduction of halide deficiency by adding external Cl- species is the most efficient way to produce high-quality blue-emitting Cl-PNCs. In this way, Figure 5b shows the developing of the different strategies reported along the time to obtain less-defective PNCs with improved PLQY up to 100%. For this figure we have considered only reported results of PLQY after PNCs washing/purification and not from raw PNC just after synthesis, as the washed PNCs are the ones susceptible to be incorporated in optoelectronic devices.

Concluding remarks and future perspectives

In this review, we discussed the main strategies shown in the current state-of-the-art for obtaining high-quality PNCs, with improved photophysical properties, and 100% PLQY. These strategies point out that the challenge to prepare PNCs with high optical performance, resides on a suitable repair or ligand coverage of the material surface, in order to passivate the surface defects

and reduce the non-radiative recombination centers. In this context, an efficient ligand coverage and a suitable surface stoichiometry can be reached by using adequate antisolvents during the purification stage and performing the surface restoration by using promising capping agents or salts with high capability to remove defect centers. Meanwhile, the partial Pb substitution or the use of promising protocols for PNCs synthesis are considered pivotal to suppress surface defects and favor the radiative recombination dynamics. From our point of view, strategies based on ligand passivation and the suppression of halide defects by incorporation of metal halide salts/partial Pb substitution are the most effective ways to ensure the formation of less-defective PNCs. This is because PNCs are prone to suffer the detachment of alkylammonium halide species during aging, generating a high density of halide defects to damage the material surface. In the case of iodide perovskites, the emergence of high halide deficiency causes the transformation of photoactive α-black phase to inactive yellow δ-phase, losing completely their optical properties and stability. Stable PNCs with near-unity PLQY can be achieved by filling the halide vacancies and favoring an adequate ligand coverage by (i) increasing the ligand content or (ii) using stronger binding capping agents. In this general context halide nature has to be taken into account in order to refine PLQY optimization.

We also address future opportunities (see Outstanding Questions) to consider in the development of novel protocols for PNCs preparation such as synthesis parameters, the organic, inorganic or hybrid nature of the material, and the substitution of conventional ligands by potential candidates to mediate PNCs growth with remarkable PL features. At this point, it is essential to understand how the functional groups from promising capping agents can offer a stronger binding to the PNCs core without requiring additional post-treatments. Future studies are needed for conducting the synthesis of unity-PLQY lead-free PNCs by supporting the total Pb replacement with substitutes that guarantee a less defective material. Moreover, the choice of hydrophobic ligand could be optimized not only for the successfully passivation of the NCs surface, but also to increase the stability in water and the relative application. These definitively are the big goals to boost the efficiencies and the commercialization of perovskite-based technologies.

Conflicts of interest

The authors declare no competing interests.

Acknowledgements

Financial support from the European Research Council (ERC) via Consolidator Grant (724424 No-LIMIT), Ministry of Science and Innovation of Spain under Project STABLE PID2019-

107314RB-I00 and Generalitat Valenciana via Prometeo Grant Q-Devices (Prometeo/2018/ 098) is gratefully acknowledged.

Glossary

Capping ligands: also known as stabilizing agents, are organic molecules, surfactants or polymers employed to coat nanoparticles. These agents show an amphiphilic structure, where the polar head coordinates with the particle core, while the non-polar tail interact with the external medium. Capping ligands are useful for hindering the aggregation and controlling the material size and shape, and also to passive surface defects.

Carrier lifetime: is referred as the average time that an excess of minor carriers takes to recombine. This process can be performed via band-to-band, trap-to-band and Auger recombination pathways.

Full width at half maximum: is defined to the width of a distribution curve measured between two points on the *y*-axis which are in the half of the maximum value.

Halide perovskite nanocrystals (PNCs): are a class of semiconductors (with size ~2-20 nm large) with an ABX_3 type structure, where in most of the studies A= Cs^+, MA^+, FA^+; B= Pb^{2+}, Sn^{2+} and X= Cl^-, Br^-, I^-, or combinations, exhibiting unique features different to other conventional nanosized materials or quantum dots. These outstanding characteristics are based mainly on a higher absorption coefficient, longer diffusion length, higher carrier mobility, tolerant-to-defect structure, and tunable optical properties by controlling quantum-size effects. To highlight, some of these PNCs can emit brightly without performing ligand passivation, and they can be good bright emitters even under larger particle size. This fact makes that PNCs showing polydispersity can provide narrow linewidths. By attending these attributes and the low-cost and facile synthesis, the commercial interest to use PNCs has increased in optoelectronic applications such as light-emitting diodes, photodetectors, solar cells, among others.

Non-radiative recombination: is referred to the trap-to-band transitions, where the electrons in the CB are trapped in new energy states formed into the band gap of the material by a dopant or a structural defect. The generated energy is released as a lattice vibration, forming a phonon instead a photon. Unlike radiative recombination, this process reduces the PLQY and increases the thermal energy into the material.

Perovskite black phase: is referred as the photoactive polymorph of iodide perovskites, formed by the dynamic motion of [PbI_6] octahedra to form a highly symmetric crystal structure. Depending on the distortion of octahedra, different optically phases such as α-, β- and γ- phases are obtained.

Photoluminescence quantum yield (PLQY): is an optical property measuring the number of photons emitted in fraction to the number of photons adsorbed. PLQY can be calculated in a range between 0 – 100%, being unity the indication that a high-quality material, with reduced density of defects, can emit the same number of collected photons.

Radiative recombination: is referred to the band-to-band transitions, where the electrons in a high energy level (conduction band, CB) decay to a lower energy empty level (valence band, VB), emitting the generated energy in form of photon.

Schottky defects: In ionic solids, are referred to the structural imperfections generated by atomic vacant positions. These vacancies are created by the movement of opposite ions from the interior to the material surface, leaving opposite charged vacancies. Schottky defects are produced stoichiometrically to preserve the electroneutrality in the solid.

Surface passivation: is referred to the formation of a protective shell layer on the material surface through a chemical reaction, which support the reduction of surface defects, improves, and preserves the intrinsic properties of the material. In this context, a passivated material is less affected by the external environment.

Yellow δ-phase: is referred to the non-photoactive polymorph of iodide presenting a non-perovskite crystalline structure formed by the destabilization of the perovskite structure at room temperature. This phase shows a non-perovskite structure with double-chains of non-corner-sharing [PbI_6] octahedra.

References

1. Protesescu, L. *et al.* (2015) Nanocrystals of Cesium Lead Halide Perovskites (CsPbX3, X = Cl, Br, and I): Novel Optoelectronic Materials Showing Bright Emission with Wide Color Gamut. *Nano Letters* 15 (6), 3692-3696
2. Gualdrón-Reyes, A. F. *et al.* (2020) Unravelling the Photocatalytic Behavior of All-Inorganic Mixed Halide Perovskites: The Role of Surface Chemical States. *ACS Applied Materials & Interfaces* 12 (1), 914-924

3. Du, X. *et al.* (2017) High-quality CsPbBr3 perovskite nanocrystals for quantum dot light-emitting diodes. *RSC Advances* 7 (17), 10391-10396
4. Liu, F. *et al.* (2017) Colloidal Synthesis of Air-Stable Alloyed CsSn1–xPbxI3 Perovskite Nanocrystals for Use in Solar Cells. *Journal of the American Chemical Society* 139 (46), 16708-16719
5. Hassanabadi, E. *et al.* (2020) Ligand & Band Gap Engineering: Tailoring the Protocol Synthesis for Achieving High-Quality CsPbI3 Quantum Dots. *Nanoscale* 12, 14194-14203
6. Grisorio, R. *et al.* (2019) Exploring the surface chemistry of cesium lead halide perovskite nanocrystals. *Nanoscale* 11 (3), 986-999
7. Nedelcu, G. *et al.* (2015) Fast Anion-Exchange in Highly Luminescent Nanocrystals of Cesium Lead Halide Perovskites (CsPbX3, X = Cl, Br, I). *Nano Letters* 15 (8), 5635-5640
8. Park, D. H. *et al.* (2018) Facile synthesis of thermally stable CsPbBr3 perovskite quantum dot-inorganic SiO2 composites and their application to white light-emitting diodes with wide color gamut. *Dyes and Pigments* 149, 246-252
9. Lu, M. *et al.* (2018) Highly Flexible CsPbI3 Perovskite Nanocrystal Light-Emitting Diodes. *ChemNanoMat* 5 (3), 313-317
10. Shen, X. *et al.* (2019) Zn-Alloyed CsPbI3 Nanocrystals for Highly Efficient Perovskite Light-Emitting Devices. *Nano Letters* 19 (3), 1552-1559
11. Zhang, C. *et al.* (2020) Core/Shell Perovskite Nanocrystals: Synthesis of Highly Efficient and Environmentally Stable FAPbBr3/CsPbBr3 for LED Applications. *Advanced Functional Materials* 30 (31), 1910582
12. Chiba, T. *et al.* (2018) Anion-exchange red perovskite quantum dots with ammonium iodine salts for highly efficient light-emitting devices. *Nature Photonics* 12 (11), 681-687
13. Lin, K. *et al.* (2018) Perovskite light-emitting diodes with external quantum efficiency exceeding 20 per cent. *Nature* 562 (7726), 245-248
14. Li, F. *et al.* (2019) Perovskite Quantum Dot Solar Cells with 15.6% Efficiency and Improved Stability Enabled by an α-CsPbI3/FAPbI3 Bilayer Structure. *ACS Energy Letters* 4 (11), 2571-2578
15. Xue, J. *et al.* (2018) Surface Ligand Management for Stable FAPbI3 Perovskite Quantum Dot Solar Cells. *Joule* 2 (9), 1866-1878
16. Sanehira, E. M. *et al.* (2017) Enhanced mobility CsPbI3 quantum dot arrays for record-efficiency, high-voltage photovoltaic cells. *Science Advances* 3 (10), eaao4204
17. Zhang, L. *et al.* (2020) All-Inorganic CsPbI3 Quantum Dot Solar Cells with Efficiency over 16% by Defect Control. *Advanced Functional Materials*, 2005930
18. Hao, M. *et al.* (2020) Ligand-assisted cation-exchange engineering for high-efficiency colloidal Cs1−xFAxPbI3 quantum dot solar cells with reduced phase segregation. *Nature Energy* 5 (1), 79-88
19. Cardenas-Morcoso, D. *et al.* (2019) Photocatalytic and Photoelectrochemical Degradation of Organic Compounds with All-Inorganic Metal Halide Perovskite Quantum Dots. *The Journal of Physical Chemistry Letters* 10 (3), 630-636
20. Xu, Y.-F. *et al.* (2017) A CsPbBr3 Perovskite Quantum Dot/Graphene Oxide Composite for Photocatalytic CO2 Reduction. *Journal of the American Chemical Society* 139 (16), 5660-5663
21. Pavliuk, M. V. *et al.* (2018) Hydrogen evolution with CsPbBr3 perovskite nanocrystals under visible light in solution. *Materials Today Communications* 16, 90-96
22. Poli, I. *et al.* (2019) Graphite-protected CsPbBr3 perovskite photoanodes functionalised with water oxidation catalyst for oxygen evolution in water. *Nature Communications* 10 (1), 2097
23. Chen, K. *et al.* (2017) Photocatalytic Polymerization of 3,4-Ethylenedioxythiophene over Cesium Lead Iodide Perovskite Quantum Dots. *Journal of the American Chemical Society* 139 (35), 12267-12273
24. Schmidt, L. C. *et al.* (2014) Nontemplate Synthesis of CH3NH3PbBr3 Perovskite Nanoparticles. *Journal of the American Chemical Society* 136 (3), 850-853

25. Yao, J.-S. *et al.* (2019) Few-Nanometer-Sized α-CsPbI3 Quantum Dots Enabled by Strontium Substitution and Iodide Passivation for Efficient Red-Light Emitting Diodes. *Journal of the American Chemical Society* 141 (5), 2069-2079
26. Li, F. *et al.* (2018) Postsynthetic Surface Trap Removal of CsPbX3 (X = Cl, Br, or I) Quantum Dots via a ZnX2/Hexane Solution toward an Enhanced Luminescence Quantum Yield. *Chemistry of Materials* 30 (23), 8546-8554
27. Yao, J.-S. *et al.* (2020) Suppressing Auger Recombination in Cesium Lead Bromide Perovskite Nanocrystal Film for Bright Light-Emitting Diodes. *The Journal of Physical Chemistry Letters* 11 (21), 9371-9378
28. Xing, G. *et al.* (2017) Transcending the slow bimolecular recombination in lead-halide perovskites for electroluminescence. *Nature Communications* 8 (1), 14558
29. ten Brinck, S. *et al.* (2019) Defects in Lead Halide Perovskite Nanocrystals: Analogies and (Many) Differences with the Bulk. *ACS Energy Letters* 4 (11), 2739-2747
30. Kim, Y.-H. *et al.* (2018) Charge carrier recombination and ion migration in metal-halide perovskite nanoparticle films for efficient light-emitting diodes. *Nano Energy* 52, 329-335
31. Kim, Y.-H. *et al.* (2017) Highly Efficient Light-Emitting Diodes of Colloidal Metal–Halide Perovskite Nanocrystals beyond Quantum Size. *ACS Nano* 11 (7), 6586-6593
32. Zhang, Y. *et al.* (2019) Fusing Nanowires into Thin Films: Fabrication of Graded-Heterojunction Perovskite Solar Cells with Enhanced Performance. *Advanced Energy Materials* 9 (22), 1900243
33. Yang, H. *et al.* (2018) Building bridges between halide perovskite nanocrystals and thin-film solar cells. *Sustainable Energy & Fuels* 2 (11), 2381-2397
34. Zheng, X. *et al.* (2019) Quantum Dots Supply Bulk- and Surface-Passivation Agents for Efficient and Stable Perovskite Solar Cells. *Joule* 3 (8), 1963-1976
35. Dong, Y. *et al.* (2020) Bipolar-shell resurfacing for blue LEDs based on strongly confined perovskite quantum dots. *Nature Nanotechnology* 15 (8), 668-674
36. Kim, Y.-H. *et al.* (2021) Comprehensive defect suppression in perovskite nanocrystals for high-efficiency light-emitting diodes. *Nature Photonics* 15 (2), 148-155
37. Pradhan, B. *et al.* (2020) Ultrasensitive and ultrathin phototransistors and photonic synapses using perovskite quantum dots grown from graphene lattice. *Science Advances* 6 (7), eaay5225
38. R, S. *et al.* (2020) Green to Blue Light Emitting CsPbBr3 Perovskite by Ligand Exchange and its Encapsulation by TiO2 for Tandem Effect in Photovoltaic Applications. *ACS Applied Nano Materials* 3 (6), 6089-6098
39. Jancik Prochazkova, A. *et al.* (2020) Controlling Quantum Confinement in Luminescent Perovskite Nanoparticles for Optoelectronic Devices by the Addition of Water. *ACS Applied Nano Materials* 3 (2), 1242-1249
40. Ahmed, G. H. *et al.* (2018) Giant Photoluminescence Enhancement in CsPbCl3 Perovskite Nanocrystals by Simultaneous Dual-Surface Passivation. *ACS Energy Letters* 3 (10), 2301-2307
41. Protesescu, L. *et al.* (2017) Dismantling the "Red Wall" of Colloidal Perovskites: Highly Luminescent Formamidinium and Formamidinium–Cesium Lead Iodide Nanocrystals. *ACS Nano* 11 (3), 3119-3134
42. Seth, S. *et al.* (2019) Tackling the Defects, Stability, and Photoluminescence of CsPbX3 Perovskite Nanocrystals. *ACS Energy Letters* 4 (7), 1610-1618
43. Wang, S. *et al.* (2018) Cesium Lead Chloride/Bromide Perovskite Quantum Dots with Strong Blue Emission Realized via a Nitrate-Induced Selective Surface Defect Elimination Process. *The Journal of Physical Chemistry Letters* 10 (1), 90-96
44. Ahmed, T. *et al.* (2018) Boosting the Photoluminescence of CsPbX3 (X = Cl, Br, I) Perovskite Nanocrystals Covering a Wide Wavelength Range by Postsynthetic Treatment with Tetrafluoroborate Salts. *Chemistry of Materials* 30 (11), 3633-3637
45. Almeida, G. *et al.* (2018) Role of Acid–Base Equilibria in the Size, Shape, and Phase Control of Cesium Lead Bromide Nanocrystals. *ACS Nano* 12 (2), 1704-1711

46. De Roo, J. *et al.* (2016) Highly Dynamic Ligand Binding and Light Absorption Coefficient of Cesium Lead Bromide Perovskite Nanocrystals. *ACS Nano* 10 (2), 2071-2081
47. Grisorio, R. *et al.* (2020) Insights into the role of the lead/surfactant ratio in the formation and passivation of cesium lead bromide perovskite nanocrystals. *Nanoscale* 12 (2), 623-637
48. Chen, K. *et al.* (2019) Short-Chain Ligand-Passivated Stable α-CsPbI3 Quantum Dot for All-Inorganic Perovskite Solar Cells. *Advanced Functional Materials* 29 (24), 1900991
49. Masi, S. *et al.* (2020) Stabilization of Black Perovskite Phase in FAPbI3 and CsPbI3. *ACS Energy Letters* 5 (6), 1974-1985
50. Wang, L. *et al.* (2017) Scalable Ligand-Mediated Transport Synthesis of Organic–Inorganic Hybrid Perovskite Nanocrystals with Resolved Electronic Structure and Ultrafast Dynamics. *ACS Nano* 11 (3), 2689-2696
51. Zhang, Y. *et al.* (2020) A "Tips and Tricks" Practical Guide to the Synthesis of Metal Halide Perovskite Nanocrystals. *Chemistry of Materials* 32 (13), 5410-5423
52. Swarnkar, A. *et al.* (2016) Quantum dot-induced phase stabilization of -CsPbI3 perovskite for high-efficiency photovoltaics. *Science* 354 (6308), 92-95
53. Bodnarchuk, M. I. *et al.* (2018) Rationalizing and Controlling the Surface Structure and Electronic Passivation of Cesium Lead Halide Nanocrystals. *ACS Energy Letters* 4 (1), 63-74
54. Liu, J. *et al.* (2019) Light-Induced Self-Assembly of Cubic CsPbBr3 Perovskite Nanocrystals into Nanowires. *Chemistry of Materials* 31 (17), 6642-6649
55. Chiba, T. *et al.* (2017) High-Efficiency Perovskite Quantum-Dot Light-Emitting Devices by Effective Washing Process and Interfacial Energy Level Alignment. *ACS Applied Materials & Interfaces* 9 (21), 18054-18060
56. Li, X. *et al.* (2016) CsPbX3 Quantum Dots for Lighting and Displays: Room-Temperature Synthesis, Photoluminescence Superiorities, Underlying Origins and White Light-Emitting Diodes. *Advanced Functional Materials* 26 (15), 2435-2445
57. Di Stasio, F. *et al.* (2018) High-Efficiency Light-Emitting Diodes Based on Formamidinium Lead Bromide Nanocrystals and Solution Processed Transport Layers. *Chemistry of Materials* 30 (18), 6231-6235
58. Di Stasio, F. *et al.* (2017) Near-Unity Photoluminescence Quantum Yield in CsPbBr3 Nanocrystal Solid-State Films via Postsynthesis Treatment with Lead Bromide. *Chemistry of Materials* 29 (18), 7663-7667
59. Wu, H. *et al.* (2018) Surface ligand modification of cesium lead bromide nanocrystals for improved light-emitting performance. *Nanoscale* 10 (9), 4173-4178
60. Shynkarenko, Y. *et al.* (2019) Direct Synthesis of Quaternary Alkylammonium-Capped Perovskite Nanocrystals for Efficient Blue and Green Light-Emitting Diodes. *ACS Energy Letters* 4 (11), 2703-2711
61. Huang, Y. *et al.* (2020) DDAB-assisted synthesis of iodine-rich CsPbI3 perovskite nanocrystals with improved stability in multiple environments. *Journal of Materials Chemistry C* 8 (7), 2381-2387
62. Zheng, W. *et al.* (2019) Stabilizing perovskite nanocrystals by controlling protective surface ligands density. *Nano Research* 12 (6), 1461-1465
63. Song, J. *et al.* (2018) Room-Temperature Triple-Ligand Surface Engineering Synergistically Boosts Ink Stability, Recombination Dynamics, and Charge Injection toward EQE-11.6% Perovskite QLEDs. *Advanced Materials* 30 (30), 1800764
64. Krieg, F. *et al.* (2018) Colloidal CsPbX3 (X = Cl, Br, I) Nanocrystals 2.0: Zwitterionic Capping Ligands for Improved Durability and Stability. *ACS Energy Letters* 3 (3), 641-646
65. Krieg, F. *et al.* (2019) Stable Ultraconcentrated and Ultradilute Colloids of CsPbX3 (X = Cl, Br) Nanocrystals Using Natural Lecithin as a Capping Ligand. *Journal of the American Chemical Society* 141 (50), 19839-19849
66. Pan, J. *et al.* (2017) Bidentate Ligand-Passivated CsPbI3 Perovskite Nanocrystals for Stable Near-Unity Photoluminescence Quantum Yield and Efficient Red Light-Emitting Diodes. *Journal of the American Chemical Society* 140 (2), 562-565

67. Park, S. *et al.* (2019) Correlation of near-unity quantum yields with photogenerated excitons in X-type ligand passivated CsPbBr3 perovskite quantum dots. *Nanoscale Advances* 1 (8), 2828-2834
68. Nenon, D. P. *et al.* (2018) Design Principles for Trap-Free CsPbX3 Nanocrystals: Enumerating and Eliminating Surface Halide Vacancies with Softer Lewis Bases. *Journal of the American Chemical Society* 140 (50), 17760-17772
69. Wang, H. *et al.* (2018) Emission Recovery and Stability Enhancement of Inorganic Perovskite Quantum Dots. *The Journal of Physical Chemistry Letters* 9 (15), 4166-4173
70. Liu, F. *et al.* (2017) Highly Luminescent Phase-Stable CsPbI3 Perovskite Quantum Dots Achieving Near 100% Absolute Photoluminescence Quantum Yield. *ACS Nano* 11 (10), 10373-10383
71. Koscher, B. A. *et al.* (2017) Essentially Trap-Free CsPbBr3 Colloidal Nanocrystals by Postsynthetic Thiocyanate Surface Treatment. *Journal of the American Chemical Society* 139 (19), 6566-6569
72. Lu, M. *et al.* (2019) Ammonium Thiocyanate-Passivated CsPbI3 Perovskite Nanocrystals for Efficient Red Light-Emitting Diodes. *The Journal of Physical Chemistry C* 123 (37), 22787-22792
73. Huang, G. *et al.* (2017) Postsynthetic Doping of MnCl2 Molecules into Preformed CsPbBr3 Perovskite Nanocrystals via a Halide Exchange-Driven Cation Exchange. *Advanced Materials* 29 (29), 1700095
74. Lu, C.-H. *et al.* (2020) Doping and ion substitution in colloidal metal halide perovskite nanocrystals. *Chemical Society Reviews* 49 (14), 4953-5007
75. Begum, R. *et al.* (2016) Engineering Interfacial Charge Transfer in CsPbBr3 Perovskite Nanocrystals by Heterovalent Doping. *Journal of the American Chemical Society* 139 (2), 731-737
76. Dong, Y. *et al.* (2018) Precise Control of Quantum Confinement in Cesium Lead Halide Perovskite Quantum Dots via Thermodynamic Equilibrium. *Nano Letters* 18 (6), 3716-3722
77. Mondal, N. *et al.* (2018) Achieving Near-Unity Photoluminescence Efficiency for Blue-Violet-Emitting Perovskite Nanocrystals. *ACS Energy Letters* 4 (1), 32-39
78. Mir, W. J. *et al.* (2020) Lanthanide doping in metal halide perovskite nanocrystals: spectral shifting, quantum cutting and optoelectronic applications. *NPG Asia Materials* 12 (1),
79. Kroupa, D. M. *et al.* (2018) Quantum-Cutting Ytterbium-Doped CsPb(Cl1–xBrx)3 Perovskite Thin Films with Photoluminescence Quantum Yields over 190%. *ACS Energy Letters* 3 (10), 2390-2395
80. Alam, F. *et al.* (2019) Eu2+: A suitable substituent for Pb2+ in CsPbX3 perovskite nanocrystals? *The Journal of Chemical Physics* 151 (23), 231101
81. Ji, S. *et al.* (2020) Near-Unity Red Mn2+ Photoluminescence Quantum Yield of Doped CsPbCl3 Nanocrystals with Cd Incorporation. *The Journal of Physical Chemistry Letters* 11 (6), 2142-2149
82. Parobek, D. *et al.* (2016) Exciton-to-Dopant Energy Transfer in Mn-Doped Cesium Lead Halide Perovskite Nanocrystals. *Nano Letters* 16 (12), 7376-7380
83. Yong, Z.-J. *et al.* (2018) Doping-Enhanced Short-Range Order of Perovskite Nanocrystals for Near-Unity Violet Luminescence Quantum Yield. *Journal of the American Chemical Society* 140 (31), 9942-9951
84. Cai, T. *et al.* (2018) Synthesis of All-Inorganic Cd-Doped CsPbCl3 Perovskite Nanocrystals with Dual-Wavelength Emission. *The Journal of Physical Chemistry Letters* 9 (24), 7079-7084
85. Milstein, T. J. *et al.* (2018) Picosecond Quantum Cutting Generates Photoluminescence Quantum Yields Over 100% in Ytterbium-Doped CsPbCl3 Nanocrystals. *Nano Letters* 18 (6), 3792-3799
86. Cai, T. *et al.* (2020) Mn2+/Yb3+Codoped CsPbCl3 Perovskite Nanocrystals with Triple-Wavelength Emission for Luminescent Solar Concentrators. *Advanced Science*, 2001317

87. Gualdrón-Reyes, A. F. *et al.* (2021) Engineering Sr-doping for enabling long-term stable FAPb1−xSrxI3 quantum dots with 100% photoluminescence quantum yield. *Journal of Materials Chemistry C* 9 (5), 1555-1566
88. Brown, A. A. M. *et al.* (2020) Lead Halide Perovskite Nanocrystals: Room Temperature Syntheses toward Commercial Viability. *Advanced Energy Materials*, 2001349
89. Deng, W. *et al.* (2018) Organic–inorganic hybrid perovskite quantum dots for light-emitting diodes. *Journal of Materials Chemistry C* 6 (18), 4831-4841
90. Gonzalez-Carrero, S. *et al.* (2016) The Luminescence of CH3NH3PbBr3Perovskite Nanoparticles Crests the Summit and Their Photostability under Wet Conditions is Enhanced. *Small* 12 (38), 5245-5250
91. Dai, S.-W. *et al.* (2018) Perovskite Quantum Dots with Near Unity Solution and Neat-Film Photoluminescent Quantum Yield by Novel Spray Synthesis. *Advanced Materials* 30 (7), 1705532
92. Veldhuis, S. A. *et al.* (2017) Benzyl Alcohol-Treated CH3NH3PbBr3Nanocrystals Exhibiting High Luminescence, Stability, and Ultralow Amplified Spontaneous Emission Thresholds. *Nano Letters* 17 (12), 7424-7432
93. Jancik Prochazkova, A. *et al.* (2019) Proteinogenic Amino Acid Assisted Preparation of Highly Luminescent Hybrid Perovskite Nanoparticles. *ACS Applied Nano Materials* 2 (7), 4267-4274
94. Paul, S.; Samanta, A. (2019) N-Bromosuccinimide as Bromide Precursor for Direct Synthesis of Stable and Highly Luminescent Green-Emitting Perovskite Nanocrystals. *ACS Energy Letters* 5 (1), 64-69
95. Imran, M. *et al.* (2018) Benzoyl Halides as Alternative Precursors for the Colloidal Synthesis of Lead-Based Halide Perovskite Nanocrystals. *Journal of the American Chemical Society* 140 (7), 2656-2664
96. Sun, C. *et al.* (2018) A new method to discover the reaction mechanism of perovskite nanocrystals. *Dalton Transactions* 47 (45), 16218-16224
97. Dutta, A. *et al.* (2019) Near-Unity Photoluminescence Quantum Efficiency for All CsPbX3 (X=Cl, Br, and I) Perovskite Nanocrystals: A Generic Synthesis Approach. *Angewandte Chemie International Edition* 58 (17), 5552-5556
98. Dutta, A. *et al.* (2018) Tuning the Size of CsPbBr3 Nanocrystals: All at One Constant Temperature. *ACS Energy Letters* 3 (2), 329-334
99. Chen, T. *et al.* (2020) Ionic liquid assisted preparation and modulation of the photoluminescence kinetics for highly efficient CsPbX3 nanocrystals with improved stability. *Nanoscale* 12 (17), 9569-9580
100. Grisorio, R. *et al.* (2020) A new route for the shape differentiation of cesium lead bromide perovskite nanocrystals with near-unity photoluminescence quantum yield. *Nanoscale* 12 (32), 17053-17063

Figures

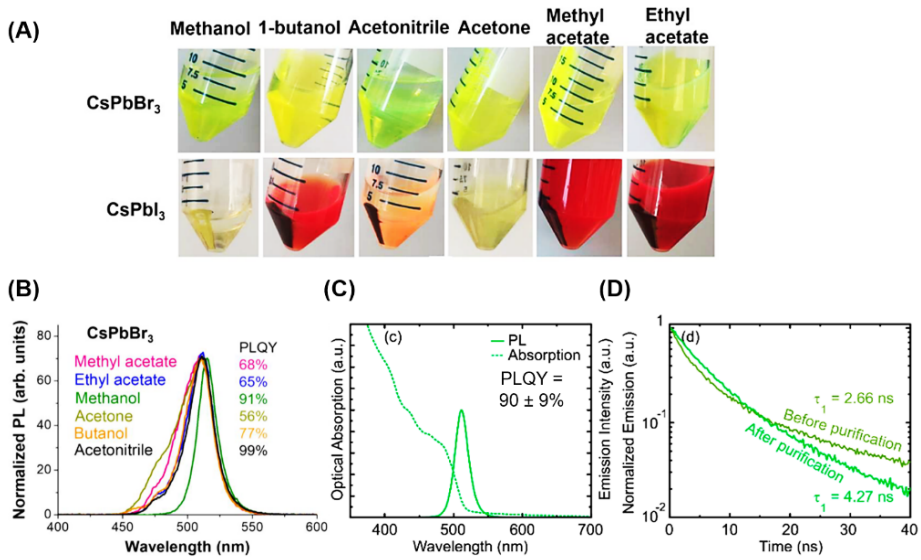

Figure 1. Purification of perovskite nanocrystals with antisolvents. (A) Photographs of $CsPbBr_3$ and $CsPbI_3$ nanocrystals dispersed in antisolvents with different polarity (Polarity increases from ethyl acetate → methanol). (B) PL spectra and PLQY of $CsPbBr_3$ nanocrystals dispersed in hexane, purified with high-polar and low-polar antisolvents. Reproduced with permission from [51]. (C) Optical absorption, PL, PLQY and (D) time-resolved PL measurements of $FAPbBr_3$ nanocrystals dispersed in toluene before and after purification OA + $PbBr_2$ + MeOAc. Reproduced with permission from [57].

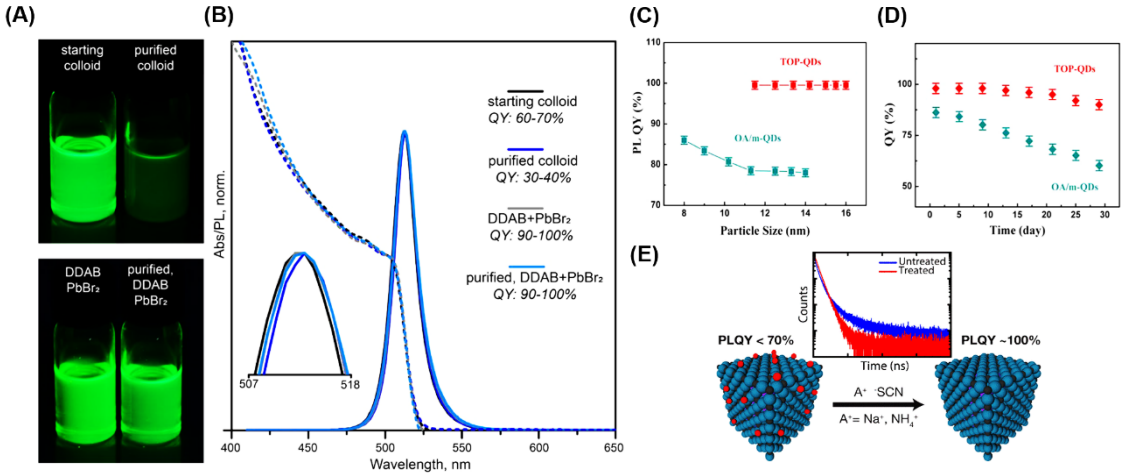

Figure 2. Repairing of the perovskite nanocrystals surface. (A) photographs of the green-luminescent colloidal solutions of $CsPbBr_3$ nanocrystals and their corresponding (B) PLQY, absorption and PL spectra before and after purification stage with acetone, in presence and absence of DDAB or DDAB + $PbBr_2$ after the post-synthetic treatment. Reproduced with permission from [53]. (C) PLQY of $CsPbI_3$ nanocrystals with and without adding TOP during their synthesis, by varying the particle size. (D) PLQY as a function of the storage time for

standard and TOP-modified $CsPbI_3$ nanocrystals. Reproduced with permission from [70]. (E) Typical PL decay and schematic representation of the surface defects reparation in $CsPbBr_3$ nanocrystals by using NaSCN and NH_4SCN. Reproduced with permission from [71].

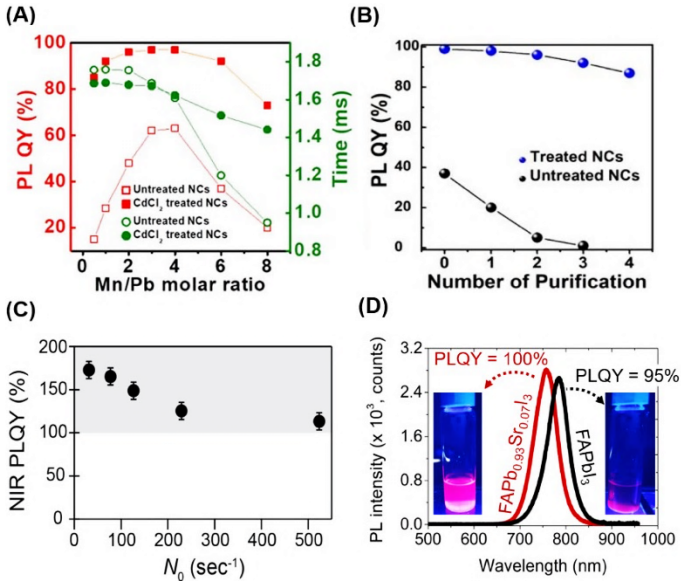

Figure 3. Partial substitution of Pb into perovskite nanocrystals. (A) PLQY and PL lifetime of the Mn^{2+}:$CsPbCl_3$ nanocrystals by varying the amount of Mn^{2+}, with and without $CdCl_2$ treatment. (B) PLQY of Mn^{2+}:$CsPbCl_3$ nanocrystals (Mn:Pb = 6:1) in function of the number of purifications with acetone before and after Cd incorporation. Reproduced with permission from [81]. (C) NIR PLQY of the 5.2 % Yb^{2+}-doped $CsPbCl_3$ nanocrystals as a function of the photoexcitation rate, carried out by varying the intensity of the excitation source (λ = 380 nm). Reproduced with the permission from [85]. (D) PL spectra and calculated PLQY of $FAPbI_3$ and $FAPb_{0.93}Sr_{0.07}I_3$ nanocrystals and their corresponding photographies under UV light (inset).

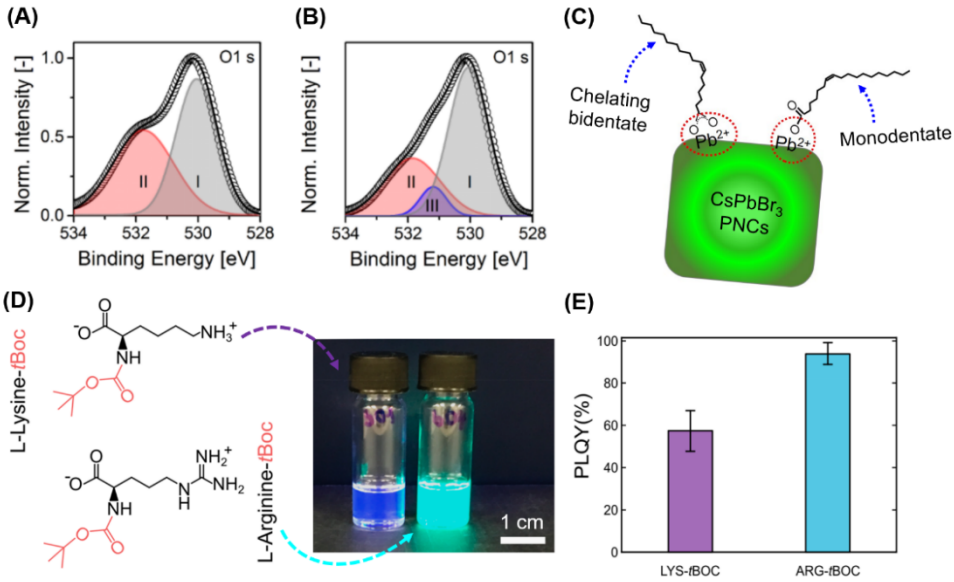

Figure 4. Characterization of high-quality perovskite nanocrystals synthesized by modifying the synthetic route based on ligand-assisted reprecipitation method (LARP). (A,B) High-resolution XPS O 1s spectra of $MAPbBr_3$ perovskite nanocrystals synthesized by LARP in presence and absence of benzyl alcohol, respectively. Regions I and III are associated to the bidentate and monodentate binding modes of the carboxylic acid (OA), while region II corresponds to the presence of O-H groups from water during perovskite synthesis. (C) Representative scheme of the bidentate and monodentate profits from carboxylate ligand bounded to the nanocrystal surface. Reproduced and adapted with the permission from [92]. (D) Photographs of the $MAPbBr_3$ perovskite nanocrystals synthesized by using L-Lysine-tBoc (LYS-tBoc) and L-Arginie-tBoc (ARG-tBoc) as capping ligands through LARP. (E) Calculated PLQY from the LYS-tBoc- and ARG-tBoc-capped $MAPbBr_3$ samples. Reproduced and adapted with the permission from [93].

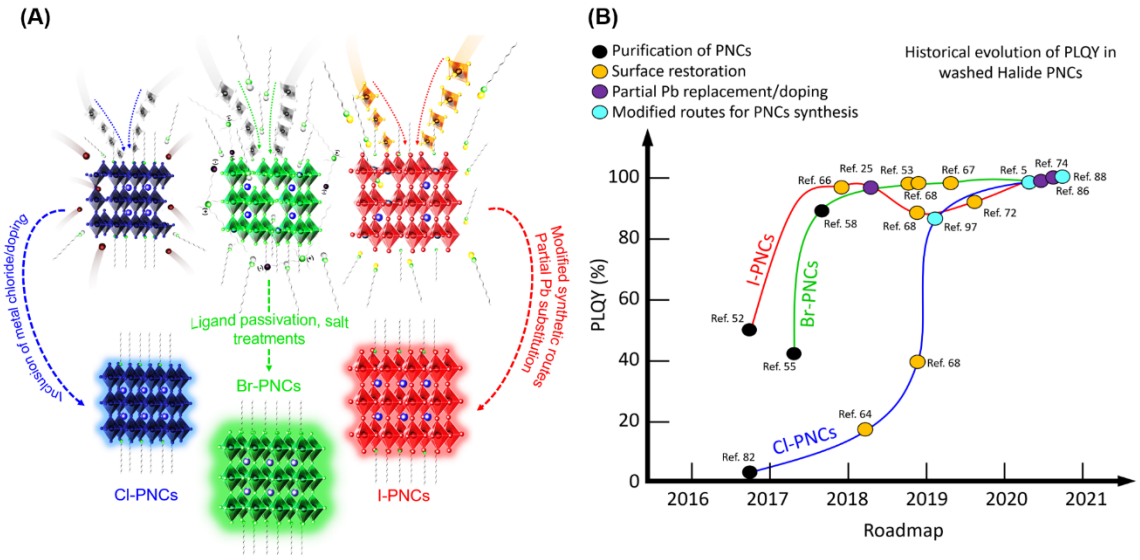

Figure 5. a) Schematic representation of the main alternatives for achieving high-quality perovskite nanocrystals with near-unity photoluminescence quantum yield, depending on the type of halide. Approaches were chosen based on the effectiveness of reduction of halide vacancies and restoration of surface defects. b) Evolution of PLQY of washed PNCs according to the different methodologies.